

## Lignin Peroxidase-Catalyzed Oxidation of Nonphenolic Trimeric Lignin Model Compounds: Fragmentation Reactions in the Intermediate Radical Cations

Enrico Baciocchi,\* Claudia Fabbri, and Osvaldo Lanzalunga\*

Dipartimento di Chimica, Università La Sapienza, P.le A. Moro, 5 I-00185 Rome, Italy

enrico.baciocchi@uniroma1.it; osvaldo.lanzalunga@uniroma1.it

Received July 22, 2003

The H<sub>2</sub>O<sub>2</sub>-promoted oxidations of the two nonphenolic β-O-aryl lignin model trimers **1** and **2**, catalyzed by lignin peroxidase (LiP) at pH = 3.5, have been studied. The results have been compared with those obtained in the oxidation of **1** and **2** with the genuine one-electron oxidant potassium 12-tungstocobalt(III)ate. These models present a different substitution pattern of the three aromatic rings, and by one-electron oxidation, they form radical cations with the positive charge, which is localized in the dialkoxyated ring as also evidenced by a pulse radiolysis study. Both the oxidations with the enzymatic and with the chemical systems lead to the formation of products deriving from the cleavage of C–C and C–H bonds in a β position with respect to the radical cation with the charge residing in the dialkoxyated ring (3,4-dimethoxybenzaldehyde (**5**) and a trimeric ketone **6** in the oxidation of **1** and a dimeric aldehyde **8** and a trimeric ketone **9** in the oxidation of **2**). These products are accompanied by a dimeric aldehyde **7** in the oxidation of **1** and 4-methoxybenzaldehyde (**10**) in the oxidation of **2**. The unexpected formation of these two products has been explained by suggesting that **1**<sup>•+</sup> and **2**<sup>•+</sup> can also undergo an intramolecular electron transfer leading to the radical cations **1a**<sup>•+</sup> and **2a**<sup>•+</sup> with the charge residing in a monoalkoxyated ring. The fast cleavage of a C–C bond β to this ring, leading to **7** from **1**<sup>•+</sup> and to **10** from **2**<sup>•+</sup>, is the driving force of the endoergonic electron transfer. A kinetic steady-state investigation of the LiP-catalyzed oxidation of the trimer **2**, the dimeric model 1-(3,4-dimethoxyphenyl)-2-phenoxy-1-ethanol (**4**), and 3,4-dimethoxybenzyl alcohol (**3**) has indicated that the turnover number (*k*<sub>cat</sub>) and the affinity for the enzyme decrease significantly by increasing the size of the model compound. In contrast, the three substrates exhibited a very similar reactivity toward a chemical oxidant [Co<sup>III</sup>W]. This suggests a size-dependent interaction of the enzyme with the substrate which may influence the efficiency of the electron transfer.

### Introduction

Lignin is a highly irregular three-dimensional biopolymer composed of oxygenated phenylpropane units linked together by different bonds, among which the most common is the so-called β–O–4 bond shown in Figure 1, where two possible phenylpropane units are represented.<sup>1,2</sup> Lignin is synthesized by plants mainly to provide strength, rigidity, and protection from oxidative processes and from attacks by microorganisms.<sup>1,3</sup>

The oxidative degradation of lignin is a process of fundamental importance not only because it can convert lignin into low molecular weight aromatic compounds, thus making this polymer a renewable source for the industrial preparation of a number of chemicals,<sup>4</sup> but also

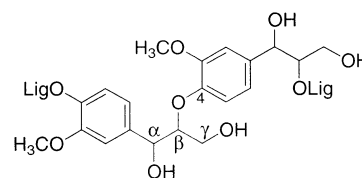


**FIGURE 1.** Two phenylpropane units of lignin linked by the β-O-4 bond.

because the selective degradation of lignin and its removal from the carbohydrate component of wood is a key step in the pulp and paper industry.<sup>5</sup>

To reduce the environmental impact and energy consumption of the lignin degradation processes, particular attention has recently been given to the natural degradation promoted by fungi, mainly of the basidiomycetous group.<sup>6–9</sup> Among the various fungi, the white rot basidi-

(1) Sarkanen, K. V. *Lignins: Occurrence, Formation, Structure and Reactions*; Sarkanen, K. V., Ludwig, C. H., Eds.; Wiley-Interscience: New York, 1971; pp 95–195.

(2) β refers to the C<sub>β</sub> carbon atom of the phenylpropane unit, –O– indicates the oxygen atom of the C<sub>β</sub>, and –4 refers to the carbon atom in the aromatic ring with C-1 carrying the propyl side chain.

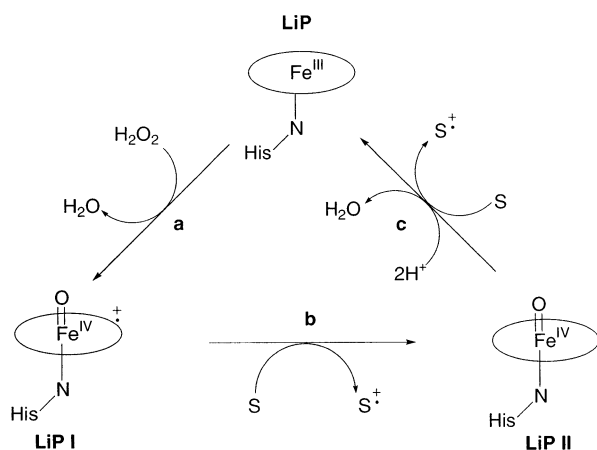
(3) Argyropoulos, D. S.; Menachem, S. B. *Biotechnology in the Pulp and Paper Industry*; Eriksson, K. E. L., Ed.; Springer-Verlag: Berlin Heidelberg, 1997; pp 127–158.

(4) Børsvik, H.-R.; Minisci, F. *Org. Process Res. Dev.* **1999**, *3*, 330.

(5) Roberts, J. C. *The Chemistry of Paper*; The Royal Society of Chemistry: Cambridge, 1996.

(6) Janshekar, H.; Fiechter, A. *Advances in Biochemical Engineering/Biotechnology*; Fiechter, A., Ed.; Springer-Verlag: Berlin, 1983; Vol. 27.

## SCHEME 1



omycetous *Phanerochaete chrysosporium* is one of the most studied;<sup>10</sup> its ligninolytic activity is due to the production of manganese peroxidase (MnP) and lignin peroxidase (LiP). LiP is a glycoprotein containing an iron(III)–protoporphyrin IX as prosthetic group, with a histidine residue (His 173) coordinated to the iron atom,<sup>11,12</sup> which differs from other heme peroxidases for its ability to oxidize aromatic nonphenolic substrates with relatively high redox potential (up to 1.4 V vs NHE).<sup>13–20</sup> It is widely accepted that the catalytic cycle of LiP involves first the reaction of the native enzyme [Por-(Fe(III))] with H<sub>2</sub>O<sub>2</sub> (Scheme 1, path a), leading to the formation of LiP compound I (LiP I), an iron(IV)–oxo porphyrin radical cation [Por<sup>•+</sup>Fe<sup>IV</sup>=O]. LiP I is the enzyme-active oxidant able to abstract one electron from the aromatic ring of the substrate, leading to [Por-Fe<sup>IV</sup>=O], LiP compound II (LiP II), and the substrate radical cation (Scheme 1, path b).<sup>12</sup> One-electron oxidation of the substrate by [Por-Fe<sup>IV</sup>=O] (Scheme 1, path c) regenerates the native enzyme.

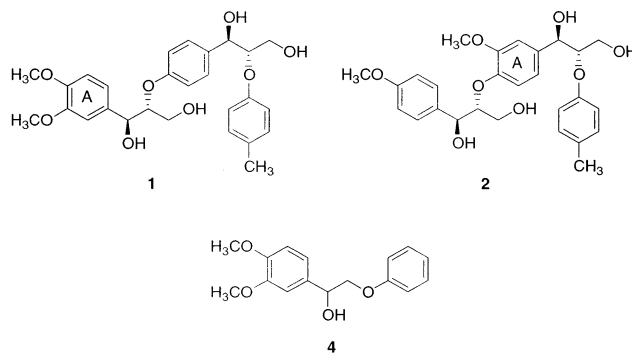
Once formed, the radical cation may undergo a number of reactions,<sup>13,14</sup> among which those involving the cleavage of C–C and C–H  $\beta$  bonds ( $\beta$  with respect to the ring

bearing the SOMO) are the most important since they should play a key role in lignin oxidative degradation.

In the past years, many studies have been carried out aimed at investigating the mechanism involved in the oxidative degradation of lignin. Because of the enormous practical problems posed by the lignin macromolecule, these studies have generally dealt with simple monomeric, dimeric, or trimeric models<sup>21</sup> containing structural motifs of the polymer.<sup>22–24</sup> Even though interesting information has been collected, the structural factors, which may play a role in determining the particular type of bond that undergoes the cleavage, have not been fully understood. One reason is that generally these models contained aromatic rings similarly activated toward electron transfer, making it practically impossible to know the localization of the positive charge in the radical cation and hence its structure.

To overcome this problem, we have directed our attention to the nonphenolic trimeric lignin model compounds **1** and **2**, both containing two  $\beta$ -O-4 linkages, which have been synthesized as a mixture of the anti–anti diastereomers (see Experimental Section).<sup>25</sup> **1** and **2** present a substitution pattern such that upon one-electron oxidation, they should form the radical cations **1**<sup>•+</sup> and **2**<sup>•+</sup>, in which the positive charge is reasonably expected to be predominantly localized in the dialkoxy-substituted ring A.<sup>26</sup>

We felt that by knowing the structure of the radical cation, it would be possible to obtain unambiguous information on the bonds which are broken and on how the structure of the radical cation may influence the relative rate of cleavage of these bonds. Thus we undertook a products investigation of the LiP-catalyzed oxidation of **1** and **2**, and the results of the enzymatic study were compared with those obtained when **1** and **2** were reacted with the genuine one-electron oxidant K<sub>5</sub>-[Co<sup>III</sup>W<sub>12</sub>O<sub>40</sub>], from now on simply indicated as Co<sup>III</sup>W.<sup>29,30</sup> Moreover, to establish to what degree the size of the model compounds may influence the rate of the enzymatic oxidation, the kinetic enzymatic constants  $K_M$  and  $k_{cat}$  for the trimer **2**, the monomeric model 3,4-dimethoxybenzyl alcohol (**3**), and the dimeric model 1-(3,4-dimethoxyphenyl)-2-phenoxy-1-ethanol (**4**) were determined. The results were compared with kinetic data obtained in the oxidation of the same substrates with the chemical oxidant Co<sup>III</sup>W. Some pulse radiolysis experiments were also carried out, aimed at obtaining additional information on the structure of **1**<sup>•+</sup> and **2**<sup>•+</sup>. The results of this investigation are reported herewith.



(7) Eriksson, K. E. L.; Blanchette, R. A.; Ander, P. *Microbial and Enzymatic Degradation of Wood and Wood Components*; Springer-Verlag: Berlin, 1990.

(8) Levy, J. F. *Cellulose Sources and Exploitation*; Kennedy, J. F., Phillips, G. O., Williams, P. A., Eds.; Ellis Horwood: New York, 1990; pp 397–408.

(9) Pedlar, S. L.; Betts, W. B. *Cellulose Sources and Exploitation*; Kennedy, J. F., Phillips, G. O., Williams, P. A., Eds.; Ellis Horwood: New York, 1990; pp 435–442.

(10) Kersten, P. J.; Stephens, S. K.; Kirk, T. K. *Biotechnology in the Pulp and Paper Manufacture*; Kirk, T. K., Chang, H. M., Eds.; Butterworth-Heinemann: Stoneham, MA, 1990; pp 457–463.

(11) Tien, M.; Kirk, T. K. *Science* **1983**, *221*, 661.

(12) Glenn, J. K.; Morgan, M. A.; Mayfield, M. B.; Kuwahara, M.; Gold, M. H. *Biochem. Biophys. Res. Commun.* **1983**, *114*, 1077.

(13) Schoemaker, H. E. *Recl. Trav. Chim. Pays-Bas*, **1990**, *109*, 255.

(14) Labat, G.; Meunier, B. *Bull. Soc. Chim. Fr.* **1990**, *127*, 553.

(15) Hammel, K. E.; Tien, M.; Kalyanaraman, B.; Kirk, T. K. *J. Biol. Chem.* **1985**, *260*, 8348.

(16) Schoemaker, H. E.; Harvey, P. J.; Bowen, R. M.; Palmer, J. M. *FEBS Lett.* **1985**, *183*, 7.

(17) Kersten, P. J.; Tien, M.; Kalyanaraman, B.; Kirk, T. K. *J. Biol. Chem.* **1985**, *260*, 2609.

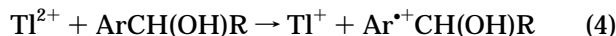
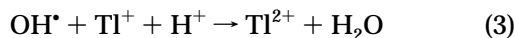
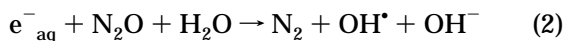
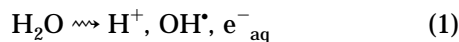
(18) Miki, K.; Renganathan, V.; Gold, M. H. *Biochemistry* **1986**, *25*, 4790.

(19) Renganathan, V.; Miki, K.; Gold, M. H. *Arch. Biochem. Biophys.* **1986**, *246*, 155.

(20) Harvey, P. J.; Floris, R.; Lundell, T.; Palmer, J.; Schoemaker, H. E.; Wever, R. *Biochem. Soc. Trans.* **1992**, *20*, 5.

## Results and Discussion

**Pulse Radiolysis Studies.** The radical cations  $1^{+\bullet}$  and  $2^{+\bullet}$  were generated from **1** and **2**, respectively, by pulse radiolysis using  $Tl^{2+}$  as the oxidant.<sup>31</sup>  $Tl^{2+}$  was produced by irradiating  $N_2O$ -saturated aqueous solutions (pH 3.5) of  $Tl_2SO_4$  (5 mM) (eqs 1–4):



The function of  $N_2O$  is to scavenge  $e_{aq}^-$ , leading to the formation of an additional hydroxyl radical (eq 2), with  $k = 9.1 \times 10^9 \text{ M}^{-1} \text{ s}^{-1}$ .<sup>34</sup>  $Tl^{2+}$  is then produced by oxidation of  $Tl^+$  by  $OH^{\bullet}$  (eq 3) with  $k = 1.2 \times 10^{10} \text{ M}^{-1} \text{ s}^{-1}$ .<sup>33</sup>  $Tl^{2+}$  reacts with alkoxyaromatics by one-electron transfer to give the corresponding radical cations (eq 4) with  $k \approx 5 \times 10^8 \text{ M}^{-1} \text{ s}^{-1}$ .<sup>35</sup> The absorption spectra obtained from **1** and **2** recorded 200  $\mu\text{s}$  after the pulse are displayed in Figures 2 and 3, respectively.

Both these spectra present absorption bands at 310 and 420 nm, that is in a region typical for aromatic radical cations and can be safely assigned to  $1^{+\bullet}$  (Figure 2) and  $2^{+\bullet}$  (Figure 3). More importantly, these spectra closely resemble the spectrum of 3,4-dimethoxybenzyl alcohol radical cation (bands at 310 and 420 nm)<sup>28</sup> while they are significantly different from the spectrum of 4-methoxybenzyl alcohol radical cation which displays two main absorption bands at 290 and 450 nm.<sup>36</sup> Thus, in line with predictions, this result indicates that in both  $1^{+\bullet}$  and  $2^{+\bullet}$  the positive charge is localized on the dialkoxylated ring. This conclusion is also supported by the observation of a very slow decay of the absorption bands of  $1^{+\bullet}$  and  $2^{+\bullet}$  (too slow to be followed in the 1-ms time scale of the experiment) as expected for a dimethoxy-substituted benzene radical cation. For example, the half-life time is 29 ms for the 3,4(MeO)<sub>2</sub>C<sub>6</sub>H<sub>3</sub>CH(OH)tBu radical cation<sup>28</sup> but only 4.6  $\mu\text{s}$  (almost 4 orders of

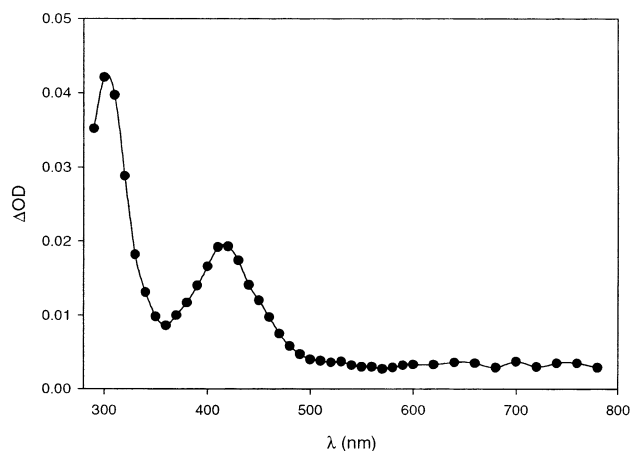


**FIGURE 2.** Time-resolved absorption spectrum observed on reaction of  $Tl^{2+}$  with **1** (0.1 mM) at  $T = 25^\circ\text{C}$ , recorded after pulse radiolysis of an  $N_2O$ -saturated aqueous solution (pH = 3.5), containing 0.5 mM  $Tl_2SO_4$ , 200  $\mu\text{s}$  after the 500-ns, 10-MeV electron pulse.

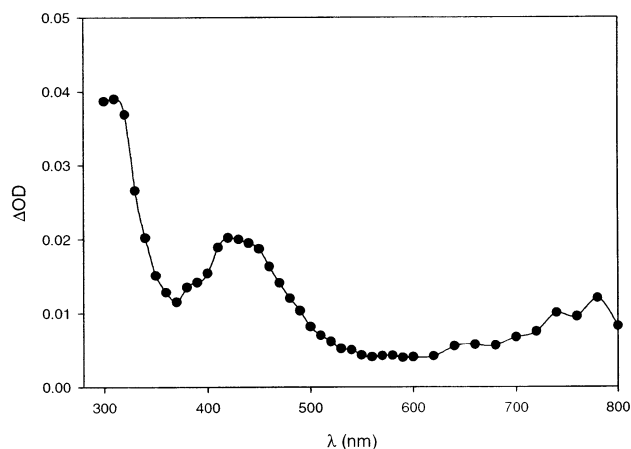


**FIGURE 3.** Time-resolved absorption spectrum observed on reaction of  $Tl^{2+}$  with **2** (0.1 mM) at  $T = 25^\circ\text{C}$ , recorded after pulse radiolysis of an  $N_2O$ -saturated aqueous solution (pH = 3.5), containing 0.5 mM  $Tl_2SO_4$ , 200  $\mu\text{s}$  after the 500-ns, 10-MeV electron pulse.

magnitude smaller) for the corresponding 4-methoxy derivative.<sup>36</sup> Another interesting observation is that the spectrum of  $2^{+\bullet}$  exhibits a broad band in the near-infrared (NIR) region of the spectrum ( $\lambda > 700 \text{ nm}$ ), which can be assigned to an intramolecular charge resonance (CR) interaction between a neutral donor ring and the charged acceptor ring in analogy with what was previously observed for the diarylmethanol radical cations.<sup>37</sup> Since the NIR band is absent in  $1^{+\bullet}$ , it would appear that only in  $2^{+\bullet}$ , where the positive charge is located in the central aromatic ring, the geometry of the system fulfills the requirement of a cofacial arrangement between donor and acceptor rings necessary for efficient charge transfer and optimum electronic coupling.<sup>38,39</sup>

**Enzymatic and Chemical Oxidation of **1** and **2**.** Oxidations of **1** or **2** with  $H_2O_2$  promoted by LiP were

(21) With these terms, it is generally indicated the number of phenylpropane units present in the model.

(22) Ten Have, R.; Teunissen, P. J. M. *Chem. Rev.* **2001**, *101*, 3397.

(23) Kirk, T. K.; Tien, M.; Kersten, P. J.; Mozuch, M. D.; Kalyanaraman, B. *Biochem. J.* **1986**, *236*, 279.

(24) Mester, T.; Ambert-Balay, K.; Ciofi-Baffoni, S.; Banci, L.; Jones, A. D.; Tien, M. *J. Biol. Chem.* **2001**, *276*, 22985.

(25) Ciofi-Baffoni, S.; Banci, L.; Brandi, A. *J. Chem. Soc., Perkin Trans. 1* **1998**, 3207.

(26) The oxidation potential of 4-methoxybenzyl alcohol<sup>27</sup> is 0.54 V higher than that of 3,4-dimethoxybenzyl alcohol.<sup>28</sup>

(27) Brown, O. R.; Chandra, S.; Harrison, J. A. *J. Electroanal. Chem.* **1972**, *38*, 185.

(28) Bietti, M.; Baciocchi, E.; Steenken, S. *J. Phys. Chem.* **1998**, *102*, 7337.

(29) Ebersson, L. *J. Am. Chem. Soc.* **1983**, *105*, 3192.

(30) Baciocchi, E.; Crescenzi, M.; Fasella, E.; Mattioli, M. *J. Org. Chem.* **1992**, *57*, 4684.

(31) Similar results have been obtained using  $Br_2^{\bullet-}$ , which is a more selective oxidant (1.63 V vs NHE)<sup>32</sup> than  $Tl^{2+}$  (2.2 V vs NHE).<sup>33</sup>

(32) Mohan, H.; Mittal, J. P. *J. Phys. Chem. A* **1997**, *101*, 10012.

(33) Schwarz, H. A.; Dodson, R. W. *J. Phys. Chem.* **1984**, *88*, 3643.

(34) Janata, E.; Schuler, R. H. *J. Phys. Chem.* **1982**, *86*, 2078.

(35) O'Neill, P.; Steenken, S.; Shulte-Frohlinde, D. *J. Phys. Chem.* **1975**, *79*, 2773.

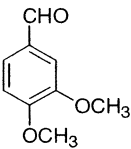
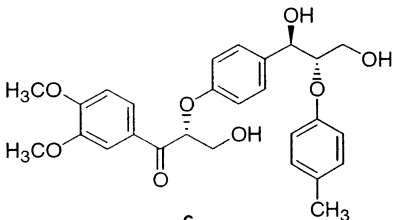
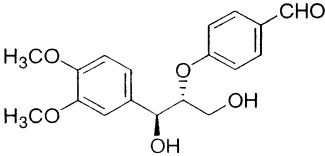
(36) Baciocchi, E.; Bietti, M.; Steenken, S. *Chem.-Eur. J.* **1999**, *5*, 1785.

(37) Bietti, M.; Lanzalunga, O. *J. Org. Chem.* **2002**, *67*, 2632.

(38) Rathore, R.; Lindeman, S. V.; Kochi, J. K. *J. Am. Chem. Soc.* **1997**, *119*, 9393.

(39) Badger, B.; Brocklehurst, B. *Trans. Faraday Soc.* **1969**, *65*, 2583.

TABLE 1. Products and Yields in the LiP/H<sub>2</sub>O<sub>2</sub>- and Co<sup>III</sup>W-Promoted Oxidation of the Lignin Model 1

Oxidizing System	Products (Yields %) <sup>a</sup>			1 (%) <sup>a</sup>
				
	5	6	7	
LiP/H <sub>2</sub> O <sub>2</sub>	9	4	11	68
Co(III)W	8	6	11	72

<sup>a</sup> Recovered starting material and yields of products are referred to the initial amount of the substrate. The average error is  $\pm 10\%$ .

carried out in 50 mM aqueous sodium tartrate buffer, pH 3.5, with 6% of acetonitrile added as cosolvent at 25 °C, and under an argon atmosphere. H<sub>2</sub>O<sub>2</sub>, equimolar with the substrate, was added gradually over 90 min using a syringe pump. Oxidations promoted by Co<sup>III</sup>W (2:1 molar ratio with the substrate) were also carried out under identical conditions for 48 h at 60 °C. After addition of an internal standard, the reaction products were analyzed by HPLC, HPLC-MS, and <sup>1</sup>H NMR. The results are in Tables 1 and 2.

The enzymatic oxidation of **1** promoted by the LiP/H<sub>2</sub>O<sub>2</sub> system leads mainly to the formation of 3,4-dimethoxybenzaldehyde (**5**), the ketone **6**, and the dimeric aldehyde **7** (Table 1). The structure of these products was determined by comparison with authentic specimens (**5** and **7**) or by NMR and MS analysis (**6**) (see Experimental Section). The same products, in similar proportions, were obtained in the oxidation of **1** induced by Co<sup>III</sup>W at pH = 3.5. Products and yields, referred to the initial amount of the substrate, are reported in Table 1, where the amount of the unreacted substrate is also indicated. The mass balance (with respect to the products containing the dimethoxylated ring) is satisfactory accounting for more than 90% of the starting material.

The oxidation of **2** promoted by the LiP/H<sub>2</sub>O<sub>2</sub> system leads mainly to the formation of the dimeric aldehyde **8**, the trimeric ketone **9**, and 4-methoxybenzaldehyde (**10**) (Table 2, comparison with authentic specimens). The same products, but in different relative amounts, were also observed in the oxidation of **2** induced by Co<sup>III</sup>W at pH = 3.5. Products and yields, referred to the initial amount of the substrate, are reported in Table 2. Also, in this case, the mass balance (with respect to the products containing the monomethoxylated ring) is good,

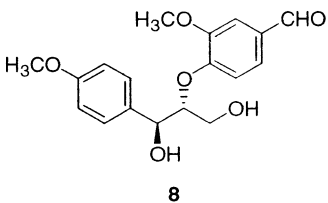
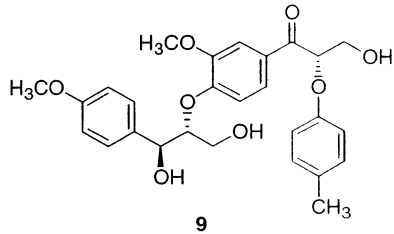
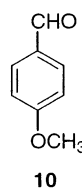
98% in the enzymatic reaction and 87% in the oxidation by Co<sup>III</sup>W.

The formation of the same products in the LiP/H<sub>2</sub>O<sub>2</sub>- and Co<sup>III</sup>W-induced reactions of both **1** and **2** indicates that the enzymatic and chemical oxidation proceed by the same mechanism. Since it is well ascertained that the oxidations promoted by Co<sup>III</sup>W take place by an electron-transfer mechanism, this observation fully confirms that also the oxidation of **1** and **2** by LiP are one-electron-transfer processes (Scheme 1), the radical cation being the key intermediate en route to the observed products.

Thus, in the oxidation of **1**, 3,4-dimethoxybenzaldehyde (**5**) should be formed, together with the carbon-centered radical **11**, by C<sub>α</sub>-C<sub>β</sub> bond cleavage in **1**<sup>•+</sup> (path a in Scheme 2), whereas C<sub>α</sub>-H bond cleavage in the same radical cation leads to the trimeric ketone **6** (paths b and d in Scheme 2).

The formation of the dimeric aldehyde **7**, the major reaction product, is more difficult to rationalize since a direct pathway leading from **1**<sup>•+</sup> to **7** would involve the breaking of a bond which is very far apart from the positively charged ring. Thus, we suggest that an additional pathway for **1**<sup>•+</sup> is an intramolecular electron transfer to give the radical cation **1a**<sup>•+</sup> where the charge is now localized in the central ring of the model (path e in Scheme 2). Cleavage of the C-C bond β to this ring (the C<sub>α</sub>-C<sub>β</sub> bond) in **1a**<sup>•+</sup> can lead to **7**. Certainly, **1a**<sup>•+</sup> is much less stable than **1**<sup>•+</sup>, but the thermodynamically uphill electron transfer is a unimolecular process and could be driven by the C-C bond cleavage reaction in **1a**<sup>•+</sup>, which is expected to be much faster in the monoalkoxylated aromatic radical cation than in **1**<sup>•+</sup>, as also clearly shown by the half-life time data reported

TABLE 2. Products and Yields in the LiP/H<sub>2</sub>O<sub>2</sub>- and Co<sup>III</sup>W-Promoted Oxidation of the Lignin Model 2

Oxidizing System	Products (Yields %) <sup>a</sup>			2 (%) <sup>a</sup>
				
LiP/H <sub>2</sub> O <sub>2</sub>	7	2	18	71
Co(III)W	9	3	3	72

<sup>a</sup> Recovered starting material and yields of products are referred to the initial amount of the substrate. The average error is  $\pm 10\%$ .

above.<sup>28,36</sup> In addition, since products coming from both  $1^{+\bullet}$  and  $1a^{+\bullet}$  are observed, and the UV-vis spectrum (Figure 2) presents only absorptions due to  $1^{+\bullet}$ , we can estimate for the  $1^{+\bullet} \rightarrow 1a^{+\bullet}$  intramolecular electron transfer a rate comparable with the decay rate of  $1^{+\bullet}$  (20–30 s<sup>-1</sup>, pulse radiolysis experiments). Now, on the basis of the Marcus equation, such a rate is consistent with an electron-transfer process endoergonic by 13 kcal mol<sup>-1</sup> (the estimated free-energy difference between the two radical cations) by assuming a quite reasonable value of 25 kcal mol<sup>-1</sup> for the intrinsic barrier  $\lambda$ .

The alternative possibility of an intermolecular electron transfer is very unlikely. In the first place, intramolecular reactions are entropically favored with respect to the intermolecular ones. In the second place, and more specifically, it has been clearly shown that *no* intermolecular electron transfer takes place between the 3,4-dimethoxybenzyl alcohol radical cation and 4-methoxymandelic acid (a system very close to those investigated by us) even though 4-methoxymandelic acid radical cation can undergo an extremely fast C–C bond cleavage.<sup>40</sup>

If the hypothesis of the intramolecular electron transfer is correct, it would result that C–C bond cleavage is the exclusive fragmentation process in  $1a^{+\bullet}$ , while in  $1^{+\bullet}$  there is competition between C–C and C–H bond cleavages. This is not surprising since it is well known that competition between C–C and C–H  $\beta$ -bond cleavage is observed in the oxidation of dimethoxylated lignin model dimers<sup>23,41</sup> whereas monomethoxylated models undergo only C–C bond cleavage.<sup>36</sup>

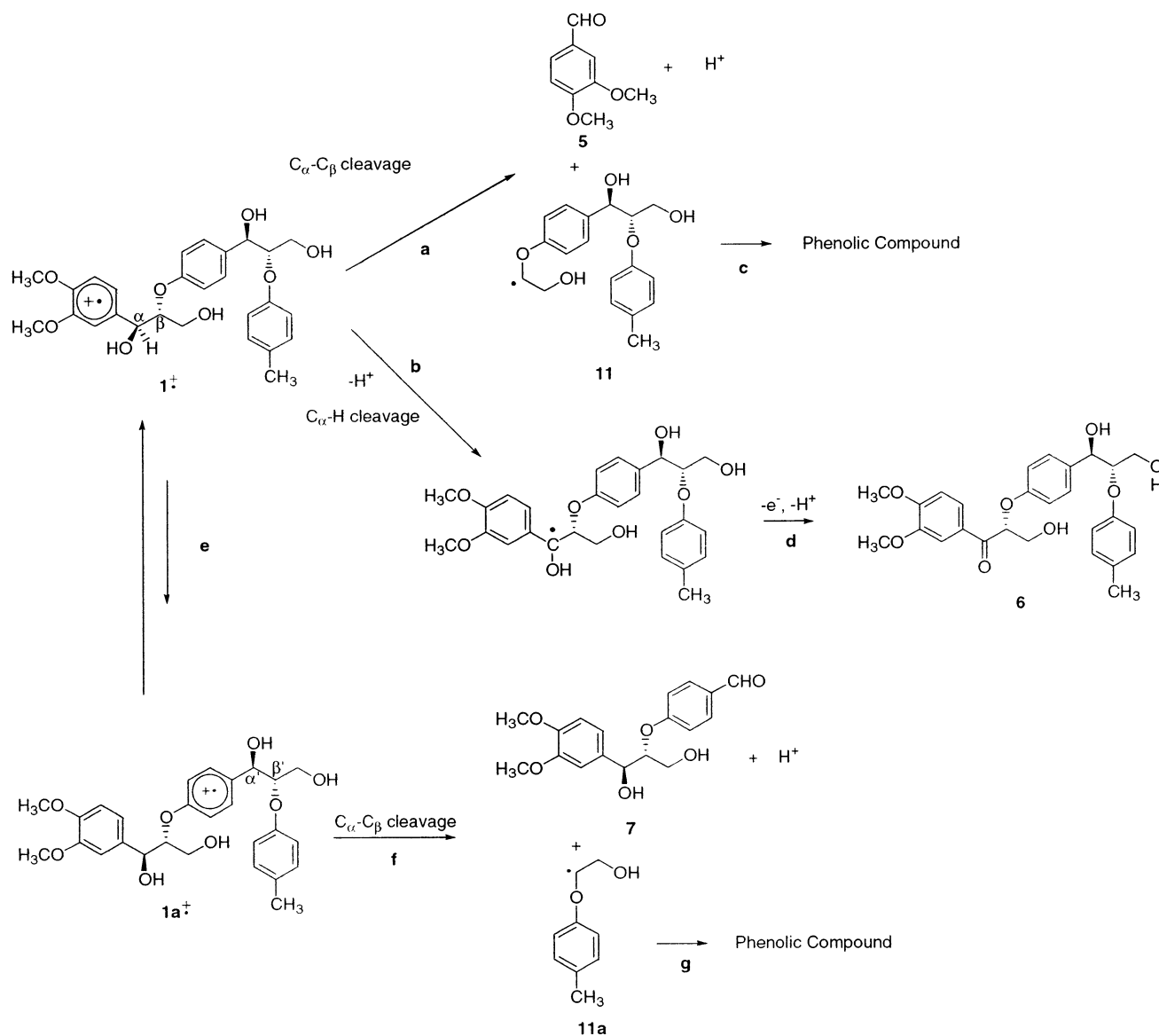
It is also important to note that the C–C bond cleavage either from  $1^{+\bullet}$  or  $1a^{+\bullet}$  is also expected to lead to the carbon-centered radicals **11** and **11a**, respectively, and to the products derived therefrom. No such products were however observed. A possible explanation is that oxidation and hydrolysis of **11** and **11a** may lead to phenolic compounds (paths c and g in Scheme 2), which are then overoxidized to water-soluble and/or polymeric species under the reaction conditions.<sup>42</sup> Fortunately, the lack of recovery of the products deriving from **11** and **11a** does not impair the mechanistic conclusions concerning the rupture modes in  $1^{+\bullet}$ . In view of the excellent mass balances noted before, there is no doubt that compounds **5**, **6**, and **7** account for the main fragmentation routes available to  $1^{+\bullet}$ .

Coming to the products from **2**, the aldehyde **8** and the ketone **9** derive from  $2^{+\bullet}$  by C<sub>α</sub>–C<sub>β</sub> and C<sub>α</sub>–H bond cleavage processes, respectively, as shown in Scheme 3 (paths a and b), analogously to what proposed for the corresponding reactions in  $1^{+\bullet}$ . In this case too, however, there is a product, namely, 4-methoxybenzaldehyde (**10**), which is by far the major product, whose formation from  $2^{+\bullet}$  is more difficult to rationalize. Accordingly, the possibility that **10** derives from the cleavage of the C<sub>α</sub>–C<sub>β</sub> bond in  $2^{+\bullet}$  is unlikely since this is a  $\gamma$  bond with respect to the positively charged ring and, at the best of our knowledge, there is no report concerning this kind of cleavage in an aromatic radical cation. Thus, we suggest that  $2^{+\bullet}$  can also undergo an intramolecular electron transfer to give the radical cation  $2a^{+\bullet}$ , a monoalkoxylated radical cation (path e in Scheme 3), which then undergoes the fast cleavage of the C<sub>α</sub>–C<sub>β</sub> bond, a  $\beta$  bond with respect to the positively charged ring.

(40) Candeias, L. P.; Harvey, P. J. *J. Biol. Chem.* **1995**, *270*, 16745.  
 (41) Bacocchi, E.; Bietti, M.; Gerini, M. F.; Lanzalunga, O.; Mancinelli, S. *J. Chem. Soc., Perkin Trans. 2* **2001**, 1506.

(42) Koduri, R. S.; Tien, M. *J. Biol. Chem.* **1995**, *270*, 22254.

## SCHEME 2



The feasibility of the  $2^{\bullet+} \rightarrow 2a^{\bullet+}$  intramolecular electron transfer can be supported by the same reasoning presented before for the  $1^{\bullet+} \rightarrow 1a^{\bullet+}$  corresponding reaction.<sup>43</sup>

As already observed for **1**, also in the oxidation of **2**, the products expected from the carbon radicals **12** and **12a** formed by C–C bond cleavage in  $2^{\bullet+}$  and  $2a^{\bullet+}$ , respectively, were not observed. The same explanation presented before (formation of easily oxidizable phenolic products, paths c and g in Scheme 3) may also hold in this case. Anyway, in this case too, the excellent mass balance noted above makes us confident that the products **8**, **9**, and **10** describe the main reaction pathways of **2**.

The observation that the LiP-catalyzed oxidation of **1** and **2** efficiently promotes the cleavage of a bond  $\beta$  to a monoalkoxylated ring is of great interest as it is well

known that LiP is unable to catalyze the oxidation of monomethoxylated substrates.<sup>13</sup> For example, LiP cannot oxidize 4-methoxymandelic acid unless a mediator is present.<sup>44,45</sup> Thus, our observation clearly indicates that the initial interaction of the enzyme with **1** or **2** concerns the more electron-rich dialkoxylated ring from which the hole can be transferred to the less activated monoalkoxylated ring. In other words, the former ring acts as an intramolecular redox mediator.

Finally, to get some information about the interaction of the lignin model trimers with the enzyme, kinetic experiments were carried out and the Michaelis–Menten constants,  $k_{\text{cat}}$  and  $K_M$ , were determined for the LiP-catalyzed oxidation of the trimeric model **2**. For comparison, we also determined  $k_{\text{cat}}$  and  $K_M$  for the oxidation of 3,4-dimethoxybenzyl alcohol (**3**), a monomeric model, and the dimeric model 1-(3,4-dimethoxyphenyl)-2-phenoxy-

(43) In this case, another mechanism leading to **10** might be an intramolecular nucleophilic attack of the alcoholic OH group to the dialkoxylated aromatic ring bearing the positive charge in  $2^{\bullet+}$  followed by ring opening of the cyclohexadienyl radical<sup>41</sup> leading to an alkoxy radical, which undergoes  $\beta$  scission. However, this mechanism should also form an isomer of **2** which has not been observed.

(44) Harvey, P. J.; Schoemaker, H. E.; Palmer, J. M. *FEBS Lett.* **1986**, *195*, 242.

(45) Baciocchi, E.; Gerini, M. F.; Lanzalunga, O.; Mancinelli S. *Tetrahedron* **2002**, *58*, 8087.

## SCHEME 3

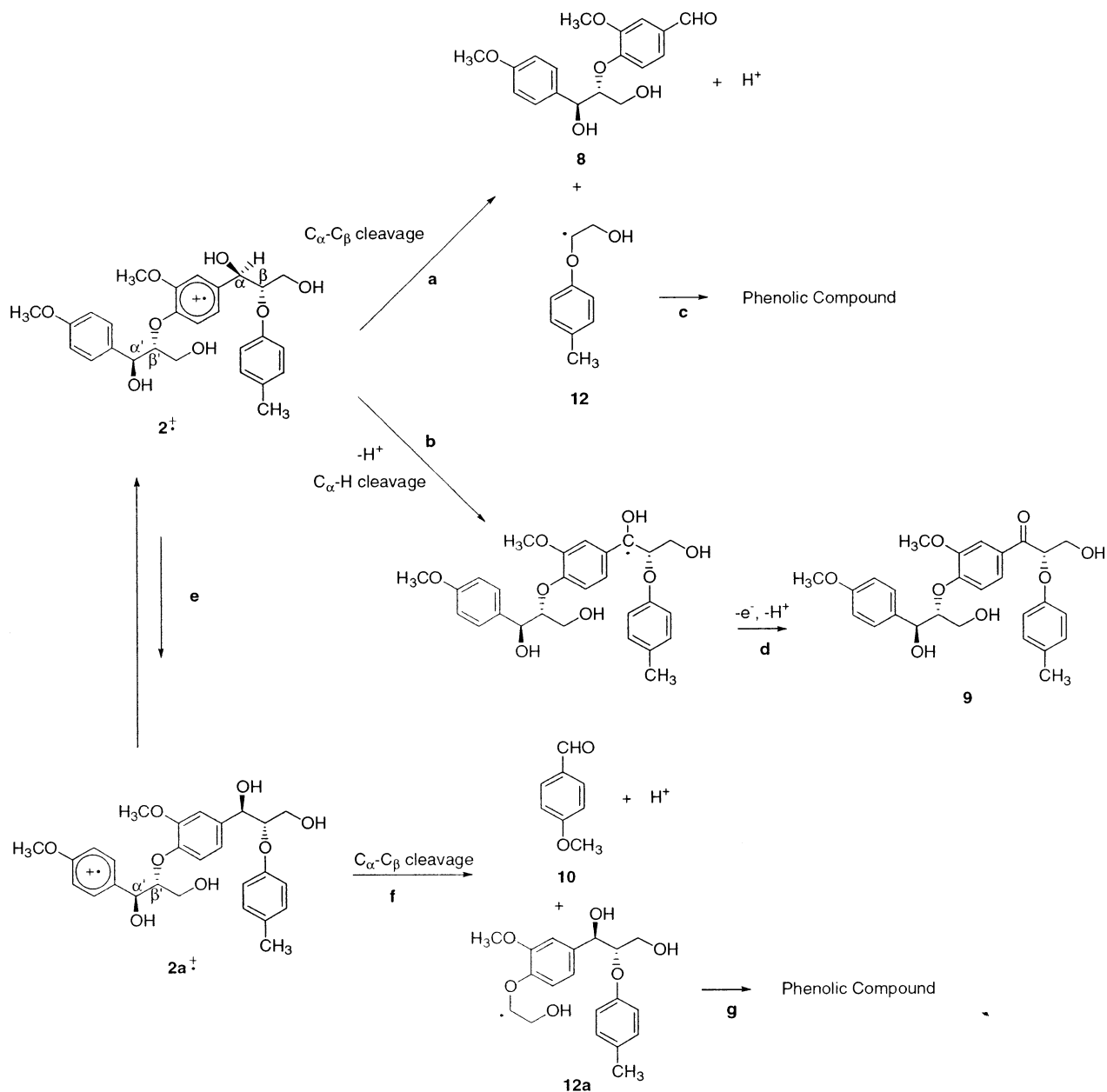


**TABLE 3. Kinetic Parameters of the Oxidation of 3, 4, and 2 Promoted by LiP/H<sub>2</sub>O<sub>2</sub> and by Co<sup>III</sup>W**

substrate	Co <sup>III</sup> W <i>k</i> (M <sup>-1</sup> s <sup>-1</sup> )	LiP/H <sub>2</sub> O <sub>2</sub>		
		<i>k</i> <sub>cat</sub> (s <sup>-1</sup> )	<i>K</i> <sub>M</sub> (mM)	<i>k</i> <sub>cat</sub> / <i>K</i> <sub>M</sub> (s <sup>-1</sup> mM <sup>-1</sup> )
<b>3</b>	0.80	1.85	0.27	6.85
<b>4</b>	0.76	0.38	0.28	1.35
<b>2</b>	0.99	0.13	0.44	0.29

1-ethanol (**4**). The results are reported in Table 3 together with kinetic data concerning the oxidation of the same models with Co<sup>III</sup>W.

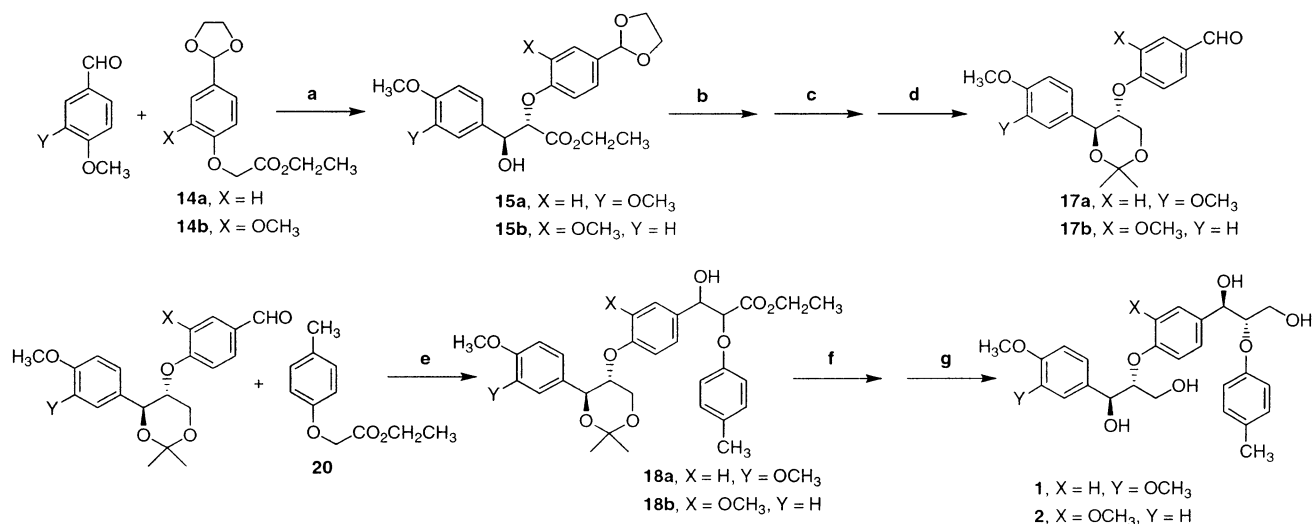
It can be noted that the efficiency of the enzymatic catalysis, as expressed by *k*<sub>cat</sub>, decreases by increasing the size of the substrate.<sup>46</sup> Thus, **3** is ca. 5 times more reactive than the dimer **4**, and **4** is ca. 3 times more reactive than the trimer **2**. In contrast, when tested

against a chemical oxidant, namely, Co<sup>III</sup>W, the three models exhibited practically the same reactivity as shown by the rate constants in Table 3. It is therefore probable that the reactivity trend observed with LiP is due to variations in the enzyme–substrate interactions related to the substrate structure. Even though **3**, **4**, and **2** exhibit a similar affinity for the enzyme (*K*<sub>M</sub> values), the way the substrate is oriented with respect to the enzyme might somewhat change with the size of the substrate itself, which might influence the efficiency of the long-range electron transfer.

Apart from the possible interpretations of the kinetic parameters in Table 3, it is remarkable that the trimeric model still exhibits a substantial reactivity. This is an

(46) Similar conclusions were established in the oxidation of phenolic lignin oligomers.<sup>47</sup>

(47) Banci, L.; Ciofi-Baffoni, S.; Tien, M. *Biochemistry* **1999**, *38*, 3205.

SCHEME 4<sup>a</sup>

<sup>a</sup> Reaction conditions: (a) LDA, THF,  $-78^{\circ}$ ; (b) NaBH<sub>4</sub>, THF, H<sub>2</sub>O; (c) PPTS, acetone, H<sub>2</sub>O; (d) TsOH, acetone; (e) LDA, THF,  $-78^{\circ}$ ; (f) NaBH<sub>4</sub>, THF, H<sub>2</sub>O; (g) PPTS, acetone, H<sub>2</sub>O.

interesting result since LiP is reported to be the peroxidase with the most restricted access to the active site,<sup>48</sup> and it seems therefore highly unlikely that a molecule as large as **2** may approach the heme edge. Thus, the significant reactivity of **2** (and probably also of the dimer **4**) might support the recent hypothesis of another, much more accessible, interaction site in LiP, located on the external surface of the enzyme and, namely, in the proximity of the residue Trp171.<sup>49,50</sup> However, direct mutagenesis and/or crystallographic studies are required to confirm this hypothesis.

## Conclusions

The results reported in this work provide significant indications about the fragmentation routes available to the intermediate radical cation in the LiP-induced oxidative degradation of trimeric model compounds **1** and **2**. The most important result is that with both models, not only the cleavage of the C–C bond  $\beta$  with respect to the dialkoxyated ring (where the positive charge is initially localized) was observed but also the cleavage of the C–C bond  $\beta$  to a monoalkoxyated ring. In fact, the major products were those coming from the latter type of cleavage. This observation was explained by suggesting the occurrence, both in **1**<sup>+</sup> and in **2**<sup>+</sup>, of an intramolecular electron transfer thereby the hole is transferred from the dialkoxyated ring (which would act as an electron transfer internal mediator) to a monoalkoxyated ring. The driving force for this energetically uphill process may be provided by the very fast cleavage of the C–C bond  $\beta$  to the positively charged monoalkoxyated ring. Apart from the mechanistic interpretation, our results indicate that in the oxidative degradation of lignin, C–C bonds, which are not in a  $\beta$  position with respect to the ring

where the positive charge is initially localized, can efficiently be broken.

A steady-state kinetic study has showed that the size of the model substrate influences the efficiency of the oxidation catalyzed by LiP, the efficiency decreasing as the model becomes larger. In contrast, the three models exhibited a very similar reactivity toward Co<sup>III</sup>W, a chemical oxidant, suggesting a size-dependent interaction of the enzyme with the substrate, which may influence the efficiency of the electron transfer. An additional observation is that with the trimeric model a substantial activity of the enzyme is still observed. Since the enzyme active site and the access channel appear almost inaccessible to the trimeric model, the above observation would support the recent suggestion of a substrate oxidation mediated by the LiP surface residue Trp171.

## Experimental Section

**Substrates.** The substrates **1** and **2** have been synthesized by condensing the three aromatic units with two aldol-type reactions as described in Scheme 4.<sup>25</sup>

The detailed description of the synthetic sequences is available in Supporting Information. The relative anti configuration of the stereocenters has been assigned on the basis of the well-documented<sup>25</sup> preferential formation of the anti product in the condensation of the lithium enolate of **14a** or **14b** with veratraldehyde or 4-methoxybenzaldehyde (step a in Scheme 4) and in the condensation of the lithium enolate of compound **20** with the dimeric aldehydes **17a** or **17b** (step e in Scheme 4). The assignment of the relative anti configuration for the two stereocenters formed in step a of Scheme 4 has been also confirmed by <sup>1</sup>H and <sup>13</sup>C NMR analysis of the 1,3-diol acetonides **17a** and **17b** (see Supporting Information).<sup>25</sup> 1-(3,4-Dimethoxyphenyl)-2-phenoxy-1-ethanol (**4**) was synthesized according to a literature procedure.<sup>41</sup>

**Products.** 4-Methoxybenzaldehyde and 3,4-dimethoxybenzaldehyde are commercially available. The dimeric aldehydes **7** and **8** have been synthesized as precursors of compounds **1** and **2**. The ketone **9** was synthesized starting from the precursor **19b** of compound **2** as described in the Supporting Information.

**Enzymatic Oxidation.** The substrate **1** or **2** (125  $\mu$ L of a solution 0.038 M in acetonitrile) and LiP (0.4 units, 0.9 nmol)

(48) Choinowski, T.; Blodig, W.; Winterhalter, K. H.; Piontek, K. J. *Mol. Biol.* **1999**, *286*, 809.

(49) Blodig, W.; Doyle, W. A.; Smith, A. T.; Winterhalter, K.; Choinowski, T.; Piontek, K. *Biochemistry* **1998**, *37*, 8832.

(50) Doyle, W. A.; Blodig, W.; Veitch, N. C.; Piontek, K.; Smith, A. T. *Biochemistry* **1998**, *37*, 15097.



were added to 2 mL of sodium tartrate buffer solution (50 mM at pH 3.5, previously degassed with argon for 15 min, under magnetic stirring in a Schlenk tube at 25 °C). H<sub>2</sub>O<sub>2</sub> (4.7 μmol) in 0.8 mL of H<sub>2</sub>O was added gradually over a period of 90 min by an infusion pump. At the end, 10 μL of a 0.1 M solution of the internal standard, 4-methoxyacetophenone, in acetonitrile was added. The reaction was quenched with methanol and analyzed by HPLC and LC-MS or extracted with dichloromethane, dried over anhydrous Na<sub>2</sub>SO<sub>4</sub>, and, after evaporation of the solvent, analyzed by <sup>1</sup>H NMR analysis. No products were observed in experiments carried out without the presence of enzyme. The reaction of **1** led to 3,4-dimethoxybenzaldehyde (**5**) and the dimeric aldehyde (**7**), which were recognized by comparison with authentic specimens. Moreover, the LC-MS spectrum of the mixture showed the presence of a compound with *M* = 482 (*M* + Na<sup>+</sup> = 505), which was assigned to the ketone **6** also on the basis of the presence in the <sup>1</sup>H NMR spectrum of signals at 7.4–7.5 δ, attributable to the protons ortho to the carbonyl group in the dimethoxylated ring. For the quantitative determination (HPLC), the response factor of **6** was taken equal to that of the ketone **9**. The reaction of **2** led to the dimeric aldehyde **8**, the ketone **9**, and 4-methoxybenzaldehyde (**10**), which were recognized by comparison with authentic specimens.

**Chemical Oxidation.** The substrate **1** or **2** (125 μL of a solution 0.038 M in acetonitrile) and Co<sup>III</sup>W (31 mg, 9.4 μmol) were added to 2 mL of sodium tartrate buffer solution (50 mM at pH 3.5, previously degassed with argon for 15 min under magnetic stirring in a Schlenk tube). The mixture was heated at 60 °C in an argon atmosphere for 48 h. At the end, 10 μL of a 0.1 M solution of the internal standard, 4-methoxyacetophenone, in acetonitrile was added. The solution was extracted with dichloromethane and dried over anhydrous Na<sub>2</sub>SO<sub>4</sub>, and the solvent was evaporated. The products were analyzed by <sup>1</sup>H NMR, HPLC, and LC-MS.

**Enzymatic Kinetics.** The kinetics were performed in a 1-mL cuvette containing 800 μL of tartrate buffer (50 mM, pH 3.5 at 25 °C). For each measure, 50 μL of a solution of LiP 4.6 mM in tartrate buffer (50 mM at pH 4) was added to the buffer followed by the solution of substrates in acetonitrile (final concentration 10%). The concentration of the substrates varied from 0.18 to 1.4 mM for **3**, from 0.11 to 0.56 mM for **4**, and from 0.10 to 0.52 mM for **2**. The reaction started by addition of 50 μL of a 0.012 M solution of H<sub>2</sub>O<sub>2</sub>. The *k*<sub>cat</sub> and *K*<sub>M</sub> values were determined at 310 nm following the formation

of products containing a carbonyl group in the α position with respect to the dialkoxylated aromatic ring, that is, 3,4-dimethoxybenzaldehyde (oxidation of **3**), 3,4-dimethoxybenzaldehyde and 1-(3,4-dimethoxyphenyl)-2-phenoxy-1-ethanone (oxidation of **4**),<sup>41</sup> and aldehyde **8** and ketone **9** (oxidation of **2**). Since two products are formed in the oxidation of **2** and **4**, the rate of the process was calculated according to the following equation  $v = (dA/dt)(1/(\epsilon_A + \epsilon_B C_B/C_A))$ , where *dA/dt* is the change of absorbance measured at 310 nm,  $\epsilon_A$  and  $\epsilon_B$  are the molar extinction coefficient of reaction products A and B at 310 nm, and *C*<sub>A</sub> and *C*<sub>B</sub> are the molar concentrations of products A and B. Kinetic parameters were not determined for the enzymatic oxidation of the trimer **1** because it was not possible to isolate the trimeric ketone **6** from the reaction mixture in a state of purity sufficient for the determination of its extinction coefficient.

**Kinetics with Co<sup>III</sup>W.** A solution of **2**, **3**, or **4** (3 μmol) and AcOK (0.6 mmol) in AcOH/H<sub>2</sub>O (70/30) was thoroughly purged with argon in a 3-mL cuvette and placed in a thermostated compartment (25 °C) of the UV-vis spectrophotometer. The reaction was started by rapid addition of 0.1 mL of a Co<sup>III</sup>W solution in AcOH/H<sub>2</sub>O (70/30) (6 mM). The rate of disappearance of cobalt(III) was followed spectrophotometrically by measuring the absorbance of Co<sup>III</sup>W at 390 nm ( $\epsilon = 1207$ ).<sup>30</sup> First-order rate constants were obtained from the plot of  $\log(A_t - A_{\text{inf}})/(A_0 - A_{\text{inf}})$  against time:  $(9.9 \pm 0.5) \times 10^{-4} \text{ s}^{-1}$  for **2**,  $(8.0 \pm 0.4) \times 10^{-4} \text{ s}^{-1}$  for **3**, and  $(7.6 \pm 0.6) \times 10^{-4} \text{ s}^{-1}$  for **4**.

**Acknowledgment.** Thanks are due to the Ministero dell'Istruzione, dell'Università e della Ricerca and the Consiglio Nazionale delle Ricerche for financial support. Pulse radiolysis experiments were performed at the Free Radical Research Facility of Daresbury, Cheshire, U.K. with the support of the European Commission through the Access to Large-Scale Facilities activity of the TMR Program. Thanks also to Prof. Suppiah Navaratnam for technical assistance.

**Supporting Information Available:** Pulse radiolysis experiments, materials, syntheses of the trimeric lignin model compounds **1**, **2**, and the ketone **9**, and <sup>13</sup>C NMR spectra of compounds **1**, **2**, **17a**, and **17b**. This material is available free of charge via the Internet at <http://pubs.acs.org>.

JO035052W